Chapter 5

Fabrication and Characterization of ZnO CQDs/ F8BT:TIPS-Pentacene Heterojunction based UV-Visible Photodetectors With/Without MoOx HTL

Chapter 5

Fabrication and Characterization of ZnO CQDs/ F8BT:TIPS-Pentacene Heterojunction based UV-Visible Photodetectors With/Without MoOx HTL

5.1. Introduction

Photodetectors for ultraviolet and visible light have been fabricated and characterized in the previous works in Chapter-2, Chapter-3, and Chapter-4. All these heterojunctions are categorized as bilayer structure. The bilayer heterojunction has drawback of poor interface due deposition second layer over the first layer. To overcome this issue, an effective and simple approach is applied by blending two organic semiconductor and formed bulk heterojunction. The blends of two different types of polymers are commonly used for fabricating flexible and light-weight devices for display devices and sensor arrays [110]. In general, the small molecule organic semiconductors show single crystalline nature in their solution processed thin films. Further, they exhibit high field-effect mobility and long-term performance stability with an efficient charge transport property suitable for optoelectronic device applications [99], [111], [112]. However, it is difficult to achieve uniformly coated large-area thin films of small-molecule on untreated substrates than the conjugate polymers due to the strong de-wetting nature of small molecule solutions [110]. In order to overcome such problems, blends of small molecule organic materials and conjugate semiconductor polymers are used to achieve reproducible polymer thin films with stable field-effect mobility of carriers [5], [6][113]. Ternary organic-inorganic semiconductors blend such as PCDTBT:PCBM:PbS QDs [81] and PCDTBT:PCBM: CdSe therapods [82] have also been reported to broaden the absorption spectral range of the films in the UV-visible photodetectors.

The chapter presents a heterojunction UV-visible photodetector by exploring the blend of F8BT (conjugate semiconductor polymer) and TIPS-P (small molecule organic semiconductor) for absorption in the visible region and ZnO CQDs for absorption in the UV region. Here, F8BT is a p-type conjugate copolymer derivative of polyfluorene containing benzothiadiazole as an electron-acceptor unit and fluorene as an electron-donor unit. Due to delocalized electrons in the conjugate polymers, F8BT has a highly effective charge carrier transport, strong stacking interface and high electrical conductivity [95]. On the other hand, the TIPS-pentacene is also a p-type small molecule organic semiconductor with good carrier mobility (> 1 cm^2/Vs) [71], [95].

In this chapter, the section 5.2 deals with the steps in fabrication process along with the proposed device structure with the relevant band diagram. Section 5.3 covers the basic optoelectronic characterization like absorbance and photoluminescence of the various semiconductor layer followed by electrical characterization and extraction of performance parameter like responsivity, EQE, and detectivity. Finally, the section 5.4 covers the basic summary and observation.

5.2. Experimental Details

All the photodetectors are fabricated on cleaned ITO-coated glass substrate with dimensions of 20 mm x 15 mm. For Device-1, thin film of ZnO CQDs was grown using spin coating unit (SPM-150LC, Germany) at 1800 rpm for 60 sec and heated at 120° C for 10 minutes using a hot-plate. The process was repeated 6 times to achieve a ~150 nm thickness of ZnO CQDs film. Finally, the ZnO CQDs thin-film was annealed at 450 °C for 30 minutes in a prebake muffle furnace. Then the F8BT: TIPS-P blend solution was spin coated on the ZnO CQDs film at 1600 rpm for 45 seconds followed by drying at 100° C in a prebake-oven

under an inert gas environment for 1h. For the Device-2 fabrication, an MoO_x film 10 nm thickness was deposited on the F8BT:TIPS-P layer using a thermal evaporation unit (FL400 SMART COAT 3.0 A, Hind High Vacuum, India). Silver (Ag) metal dots of 0.0314 cm^2 (diameter of 2 mm) were finally deposited on F8BT: TIPS-P film in Device-1 and on MoO_x film in Device-2 by the thermal evaporation method. Two device structures without and with MoO_x HTL layer along with their corresponding energy band diagrams are shown in Figure 5.1. The respective conduction band (CB) and valance band (VB) energies of ZnO QDs are assumed to be -4.36 eV and -7.59 eV; -3.5eV and -5.4eV of TIPS-P; -2.3 eV and -5.3 eV of MoO_x and -3.3 eV and -5.9 eV of F8BT[93],[95].

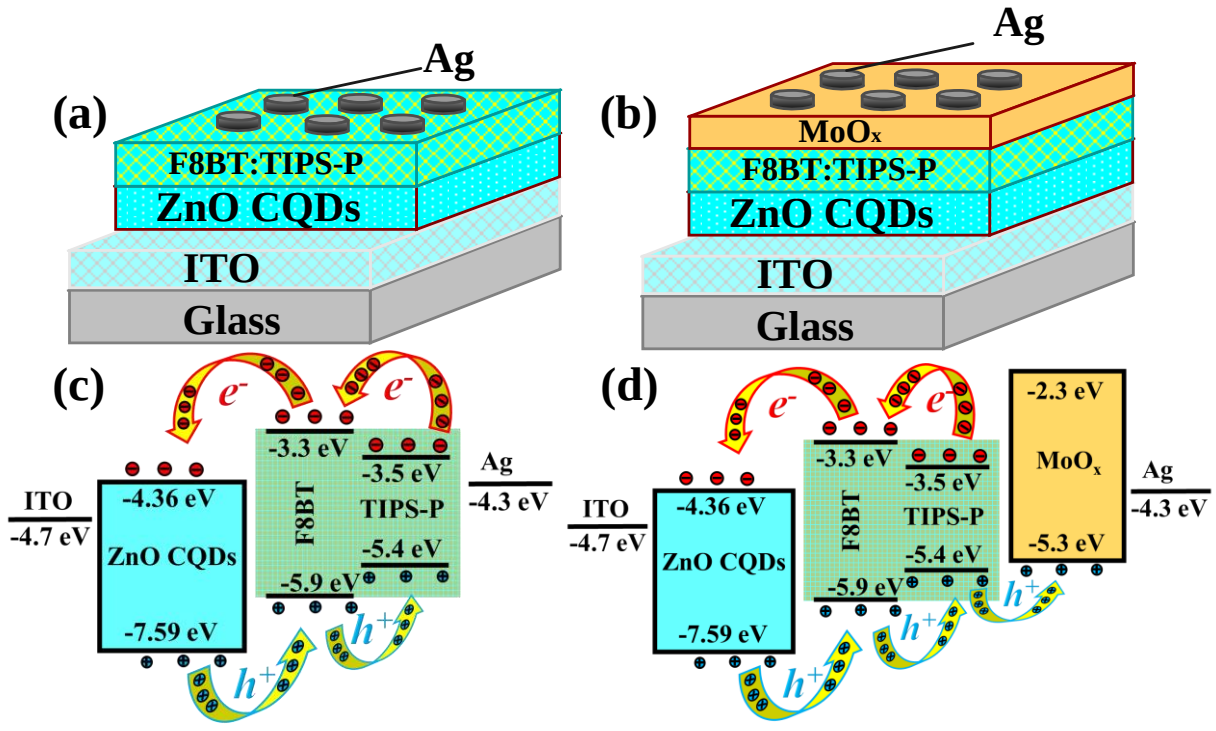

Figure 5.1. Schematic diagram of (a) Device-1 (b) Device-2 and corresponding band diagram of (c) ZnO/F8BT:TIPS-P (d) ZnO/F8BT:TIPS-P /MoOx.

5.3. Results And Discussion

5.3.1. Optical Characteristics of the Thin Films

The absorbance characteristics (measured by UV-Vis spectroscopy, V-770 from JASCO, Japan) of ZnO CQDs, F8BT, TIPS-P, MoO_x, and combined ZnO CQDs/F8BT:TIPS-P/ MoO_x films are shown in Figure 5.2 (a). The F8BT and TIPS-P films show absorbances in a wide range of the visible region while the ZnO CQDs film shows its absorbance in the UV region. The MoO_x film shows no significant effect on the combined absorbance of the ZnO CQDs/F8BT:TIPS-P/ MoO_x films in the UV as well as in the visible region due to its very small thickness of ~10 nm. The photoluminescence (PL) spectra (measured by Edinberg Spectro fluorometer FS980) of the ZnO CQDs, F8BT, TIPS-P, and combine film of ZnO CQDs/ F8BT:TIPS-P/ MoO_x films at the excitation wavelength (λex) of 375 nm are shown in Figure 5.2 (b). The PL of the ZnO CQDs and F8BT films shows peaks at ~ 440 nm and ~ 540 nm, while the PL of TIPS-P film shows no peak at the excitation wavelength of 375 nm. It is observed from Figure 5.2 (b) that the intensity of the individual PL peaks of ZnO CQDs and F8BT are decreased while the PL peak of the TIPS-P is increased in the combined PL of ZnO CQDS/ F8BT:TIPS-P/ MoO_x film. This is an interesting result representing the cascade energy transfer from the ZnO CQDs to F8BT to TIPS-P [114], [115] in the combined film. This confirms that the charge transport property of the F8BT: TIPS-P film is better than their individual charge transfer properties.

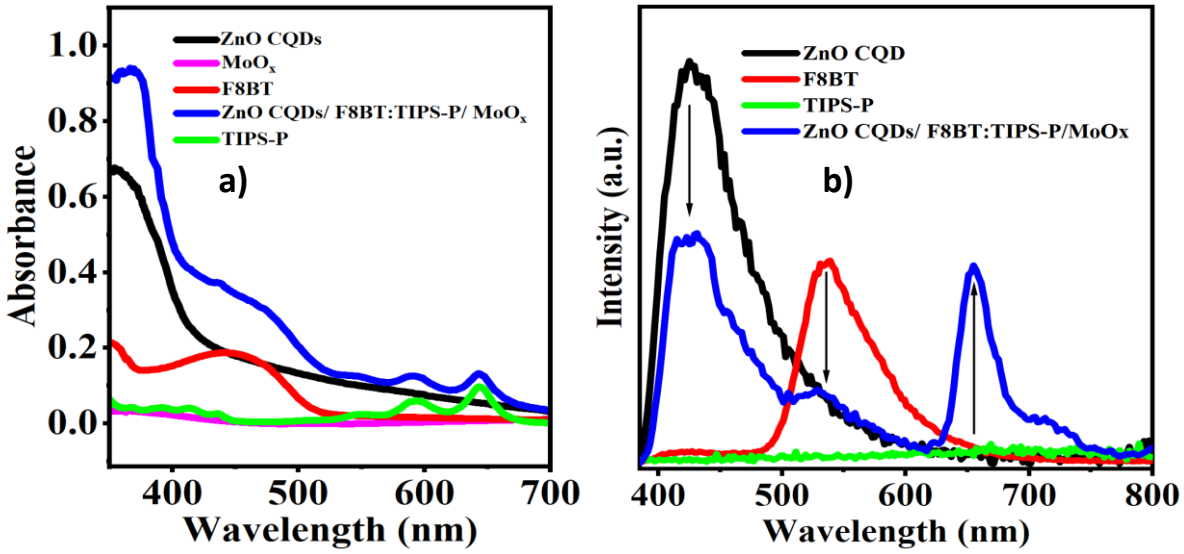

Figure 5.2 (a) Absorption spectra, and (b) Emission spectra of ZnO QDs thin film, F8BT:TIPS-P, MoOx and ZnO QDs /F8BT:TIPS-P /MoOx thin film.

5.3.2. Current-Voltage Characteristics

Figure 5.3 (a) depict the fabricated devices. The current-voltage (I-V) characteristics of Device-1 and Device-2 were measured by the parameter analyzer (B1500A, Keysight, USA) under the illumination of a white light of 55 μW/cm^2 intensity. The I-V characteristics of both the devices are compared in Figure 5.3 (b). The dark current in the forward bias is observed to be slightly larger than that under the reverse bias in Figure 5.3 (b). It confirms the rectifying nature of the n-ZnO QDs/p-F8BT:TIPS-P heterojunction. In Device 1, the dark current is ~ 35.97 μA and the current under illumination (light current) is ~ 102.62 μA. The Device-2 shows a very low dark current of 3.03 μA. The light current of Device-2 is 79.93 μA. Thus the photocurrent (i.e. light current – dark current) in Device-1 is 66.65 μA while the same in Device-2 is 76.9 μA.

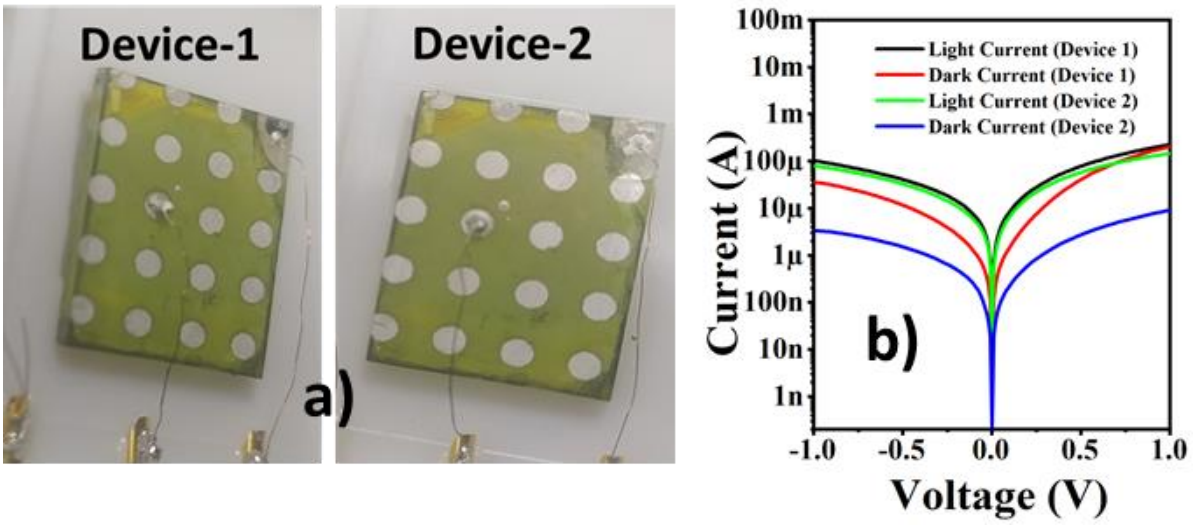

Figure 5.3 (a) Image of fabricated devices, and (b) I-V characteristic of Device-1 and Device-2.

We will now determine responsivity (R), detectivity (D*), and external quantum efficiency (EQE) of photodetector. The responsivity (R) is defined as the ratio of the photocurrent to incident optical power on the photodetector which is expressed in A/W [28], [93]. The specific detectivity (D*) represents minimum incident optical power which a photodetector can detect. EQE is defined as the ratio of the number of electrons-hole pairs collected at the external circuit to the number of photons of a particular wavelength (λ) incident on the device. The D* and EQE are calculated as[81], [93], [93], [105], [116]:

$$D^{*} = \frac{R}{\sqrt{2 \times e^{-} \times J_d}} \quad (5.1)$$

$$EQE\ \% = \frac{1240 \times R}{\lambda\,(nm)} \times 100 \quad (5.2)$$

where, e^{-} is electronic charge, J_d is the dark current density and λ is incident light wavelength in nm of the detector. The responsivity (R), and detectivity (D*) of Device-1 and Device-2 are shown in Figure 5.4 (a) and (b), respectively. The maximum values of R, D* and EQE of

the Device-1 in the UV region (at 385 nm with 17.34 μW/cm^2 intensity) are ~ 29.60 A/W, ~ 6.35 × 10^{12} Jones, and ~ 9533.50 % respectively, and in the visible region (at 470 nm with 35.94 μW/cm^2 intensity) are ~ 13.68 A/W, ~ 2.93 × 10^{12} Jones, and ~ 3609.19 % respectively. In Device-2, the maximum R, D* and EQE values are ~ 70.20 A/W, ~ 3.97 × 10^{13} Jones, ~ 22609.87 % and in UV region, and ~ 40.92 A/W, ~ 2.08 × 10^{13} Jones, ~10795.91 % and (in the visible region), respectively.

The MoOx HTL layer acts as the electron blocker but enhances hole transport. Under reverse bias, the large energy barrier for electrons at MoOx/Ag prevents the electrons from entering into the device through Ag-anode (see Figure 5.1(d)). This reduces the electron-hole recombination which, in turn, reduces the dark current and enhances the photocurrent (i.e. difference between current under illumination and dark current) of Device-2. On the other hand, a part of the photogenerated electrons gets trapped at the intrinsic defects in ZnO CQDs [3], [4]. These trapped electrons create an electrostatic field which reduces the hole injection barrier at ITO/ZnO CQDs by introducing a large interfacial band bending near the cathode in reverse

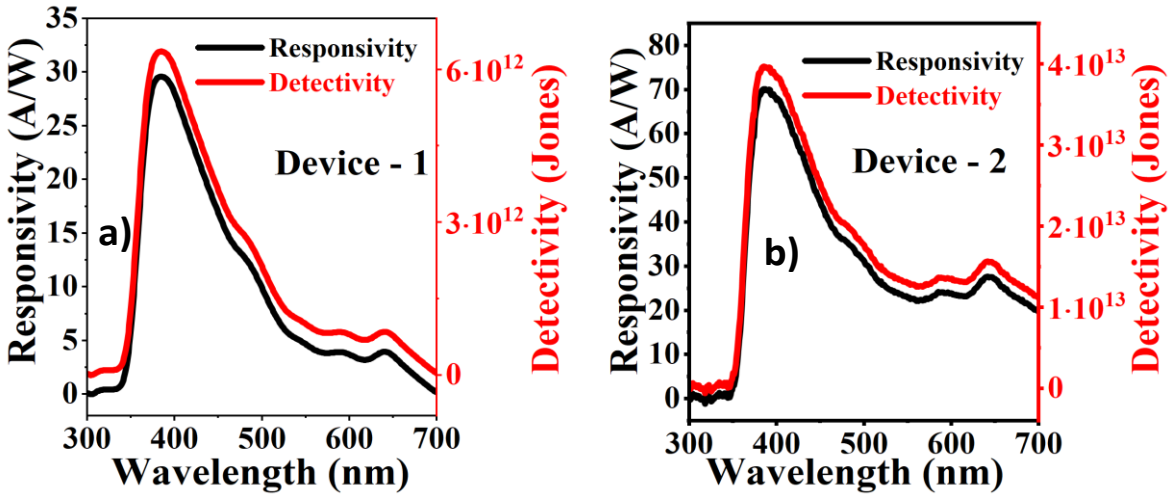

Figure 5.4 Responsivity and detectivity of (a) Device-1, and (b) Device-2.

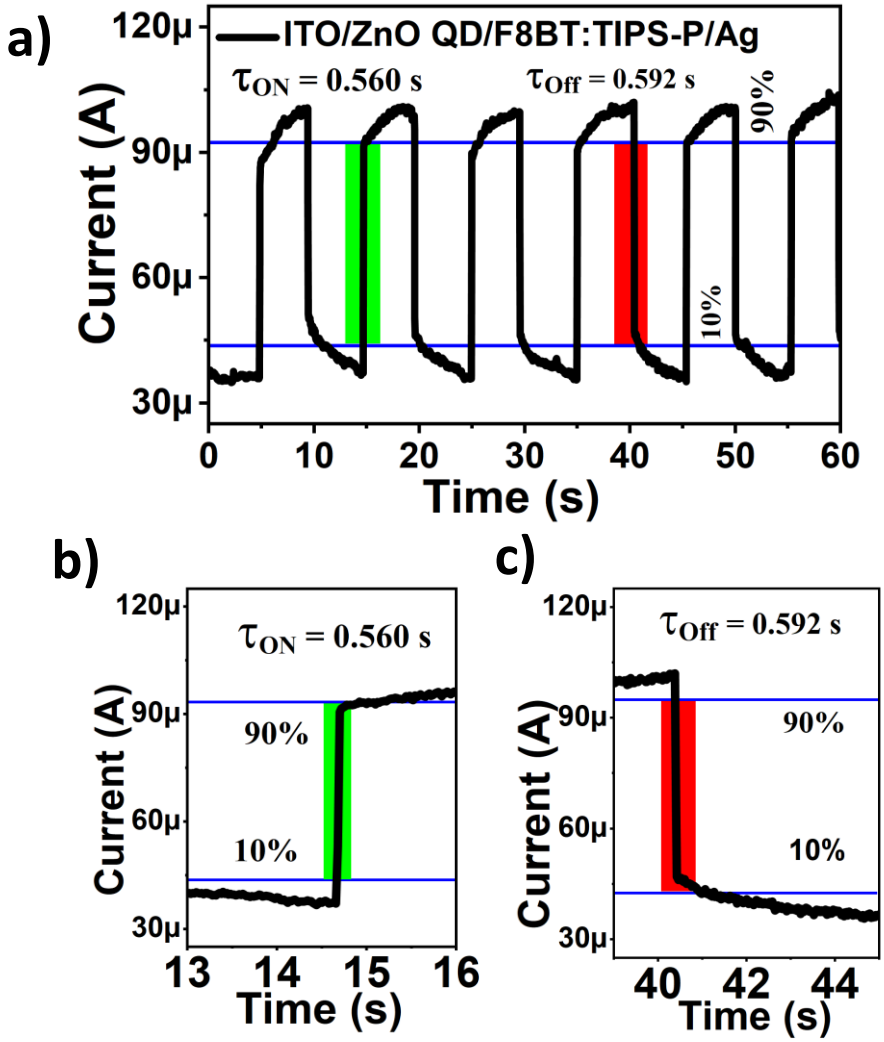

Figure 5.5. Transient response of (a) Device-1 (ITO/ZnO QDs/ F8BT:TIPS-P/Ag), (b) and (c), are their single rise and fall time response, respectively.

bias [3], [4]. This hole tunneling injection assisted by high density of trapped electrons in ZnO CQDs results in photomultiplication to enhance the EQE beyond 100%. In brief, the combined effects of reduction in dark and enhancement of photocurrent by photomultiplication drastically improve the overall performance of the Device-2. The transient responses of device-1 and device-2 are shown in Figure 5.5 and Figure 5.6. rise-time ($\boldsymbol{\tau_{on}}$) and fall-time ($\boldsymbol{\tau_{off}}$) of Device-1 are 0.560 s and 0.592 s, respectively, which are

further improved in Device-2 as 0.019 s and 0.020 s, respectively, under white light at -1 V biasing. The τ_{on} (τ_{off}) is defined as the time

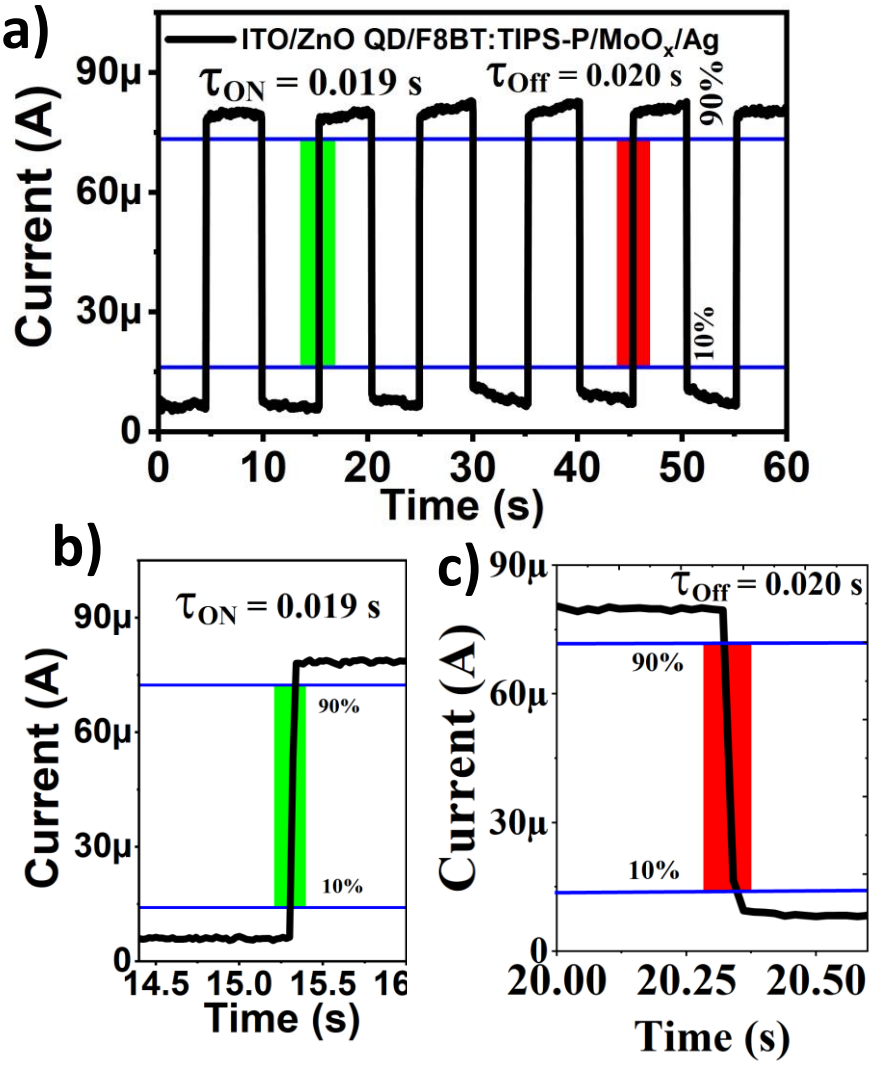

Figure 5.6. Transient response of (a) Device-2 (ITO/ ZnO QDs/ F8BT:TIPS-P/MoOx/Ag, (b) and (c), are their single rise and fall time responses, respectively.

required for changing the photocurrent from 10 % (90%) to 90 % (10%) of the maximum photocurrent immediately after turning ON (OFF) the pulsed light source. The improved transient response of Device-2 is attributed to reduced recombination and enhanced hole transportation due MoOx HTL as discussed earlier.

5.4 Conclusion

In this chapter blending of TIPS Pentacene with F8BT has yielded superior and easy processability resulting in uniform film. We also studied the effect of MoOx layer which acted as hole transport layer and electron blocking layer. The electron blocking layer helps in supression of dark current. We observed an interesting cascading charge transfer phenomenon in which the intensity of the distinct photoluminescence (PL) peaks of ZnO CQDs and F8BT declines while the PL peak of TIPS-P grows in the combined PL of ZnO CQDs/F8BT:TIPS-P/MoOx film. This fascinating result indicates a cascade energy transfer process from ZnO CQDs to F8BT and then to TIPS-P. These results validate that the F8BT:TIPS-P film has superior charge transport qualities when compared to their separate charge transfer properties.

When compared to a reference device (device without interfacial MoOx layer), the introduction of a MoOx (molybdenum oxide) hole transport layer (HTL) at a wavelength of 350 nm in the ultraviolet (UV) region resulted in improved responsivity. The maximum responsivity increased from 29.60 A/W to 70.20 A/W, while detectivity increased from 6.35×10^{12} Jones to 63.97×10^{13} Jones. Similarly device performance at 470 nm in visible region also showed improvement in responsivity from 13.68 A/W to 40.92 A/W while detectivity enhanced from and 2.93×10^{12} Jones to 2.08×10^{13} Jones, respectively, using the MoOx HTL